

Bandgap determination from individual orthorhombic thin cesium lead bromide nanosheets by electron energy-loss spectroscopy

Rosaria Brescia,^a Stefano Toso,^{b,c} Quentin Ramasse,^{*d,e} Liberato Manna,^b Javad Shamsi,^{b‡} Clive Downing,^f Arrigo Calzolari^g and Giovanni Bertoni^{*g,h}

^a Electron Microscopy Facility, Istituto Italiano di Tecnologia, Via Morego 30, 16163 Genova, Italy

^b Nanochemistry Department, Istituto Italiano di Tecnologia, Via Morego 30, 16163 Genova, Italy

^c International Doctoral Program in Science, Università Cattolica del Sacro Cuore, 25121 Brescia, Italy

^d SuperSTEM, SciTech Daresbury Science and Innovation Campus, Keckwick Lane, Daresbury WA4 4AD, UK

^e School of Chemical and Process Engineering & School of Physics, University of Leeds, Leeds LS29JT, UK

^f The Advanced Microscopy Laboratory, CRANN, Trinity College Dublin (TCD), Dublin, Ireland

^g CNR – Istituto Nanoscienze, Via Campi 213/A, 41125 Modena, Italy

^h IMEM – CNR, Istituto dei Materiali per l'Electronica e il Magnetismo, Parco Area delle Scienze 37/A, 43124 Parma, Italy

*corresponding authors: giovanni.bertoni@cnr.it, qmramasse@superstem.org

‡present address: Cavendish Laboratory, University of Cambridge, 19 JJ Thomson Avenue, Cambridge CB3 0HE, UK.

Electronic Supplementary Information

1. Check for visible structural damage at 200 kV in ADF-STEM imaging.

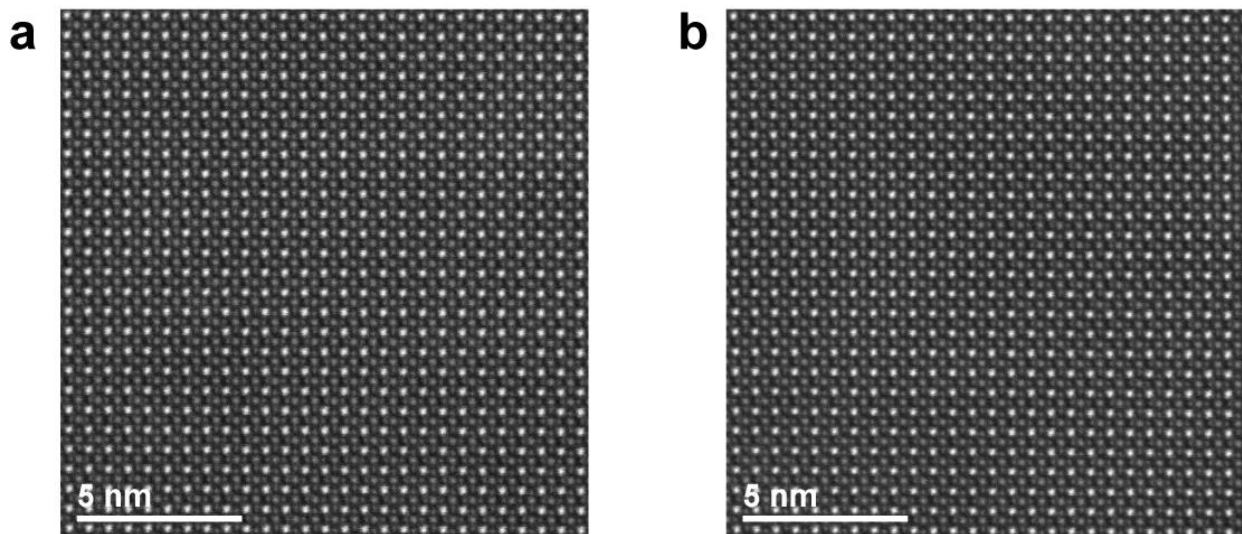


Figure S1. Two ADF-STEM raw images (1024×1024 pixels, $16 \text{ nm} \times 16 \text{ nm}$) taken in sequence on a CsPbBr_3 thick nanosheet at 200 kV with a probe current of 40 pA. (a) First scan (pixel dwell time $10 \mu\text{s}$), (b) second scan (pixel dwell time $20 \mu\text{s}$). The two images look similar with no evidence of damage induced during the scans.

2. Evidence of structural damage at 60 kV in ADF-STEM imaging.

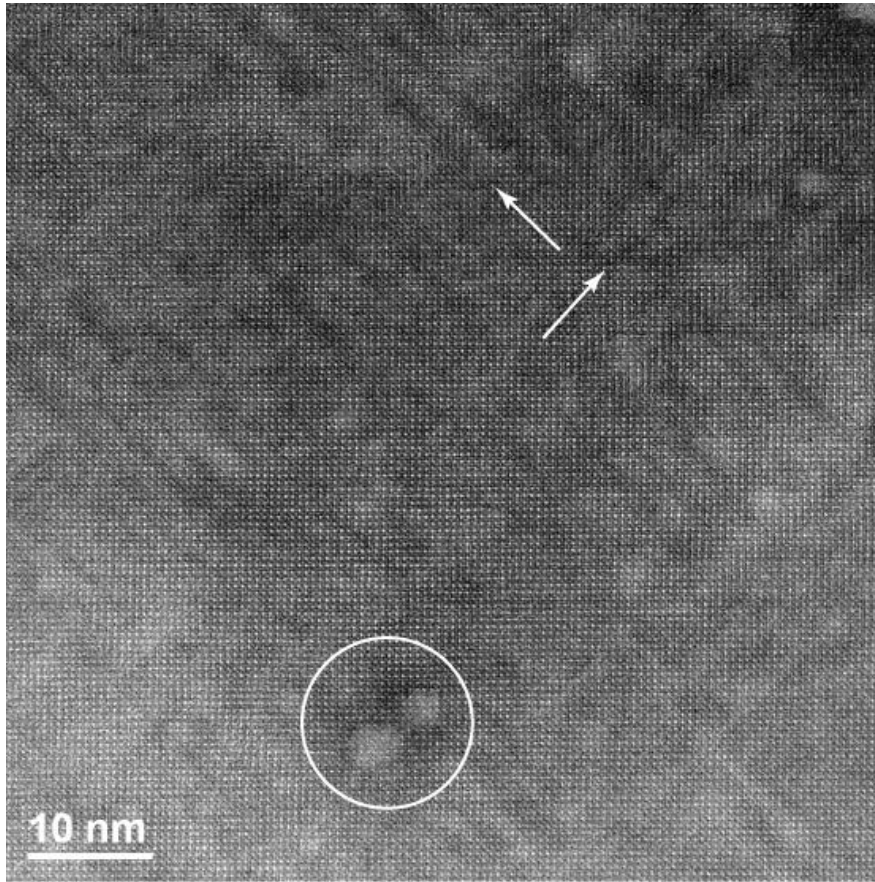


Figure S2. ADF-STEM image acquired at 60 kV after EELS exposure at high current (~ 35 pA). Evidences of damage are clearly visible, as dark regions of line defects along the [100] and [010] directions of the orthorhombic structure (white arrows), and bright round clusters (white circle). Both are probably the results of Pb diffusion and segregation due to irradiation.¹

3. Results from density functional calculations (DOS).

	a (nm)	b (nm)	c (nm)
bulk	0.8162	0.8518	1.1891
multilayer (1-16L)	0.8162	0.8518	11.2000

Table T1. Cell size for the bulk CsPbBr₃ and multilayer ($N = 1-16$) used in DFT calculations.

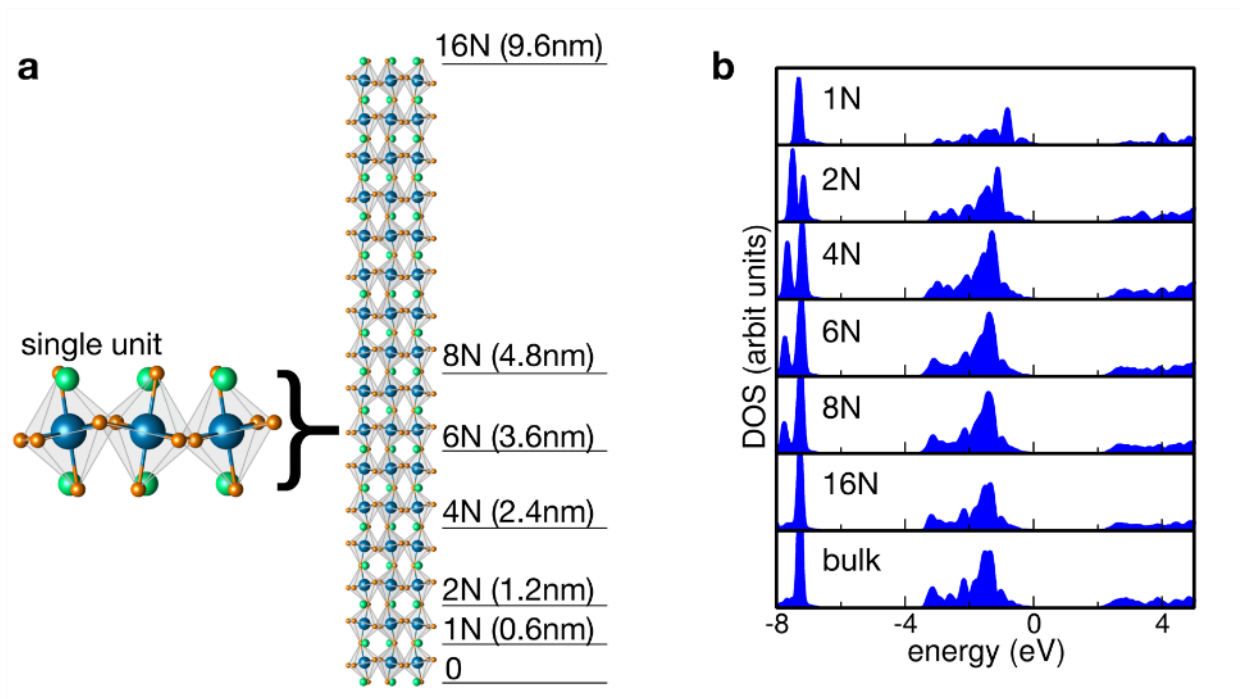


Figure S3. (a) Atomic geometries of multilayer ($N = 1-16$) structures discussed in the main text. (b) Calculated DOS for selected multilayers ($N = 1-16$). Bulk DOS (bottom panel) is included for comparison. Zero energy reference is set to the top of valence band of each system.

4. Low magnification TEM analysis of the nanosheets.

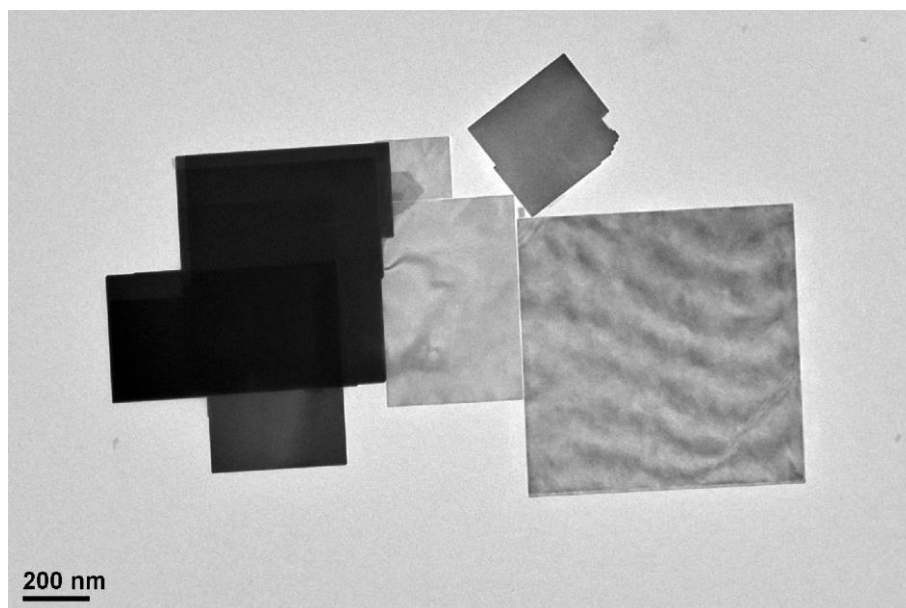


Figure S4. Bright-field TEM image at 100 kV of the nanosheets (NSs) of different thickness. Thick oriented sheets are darker, as the ones on the left region of the image. The lateral extension of the NSs can reach approximately 1 μm . This image was collected on a JEOL JEM-1011 TEM (Electron Microscopy Facility of IIT, Genova, Italy).

5. Cubic structure and orthorhombic structure of CsPbBr₃.

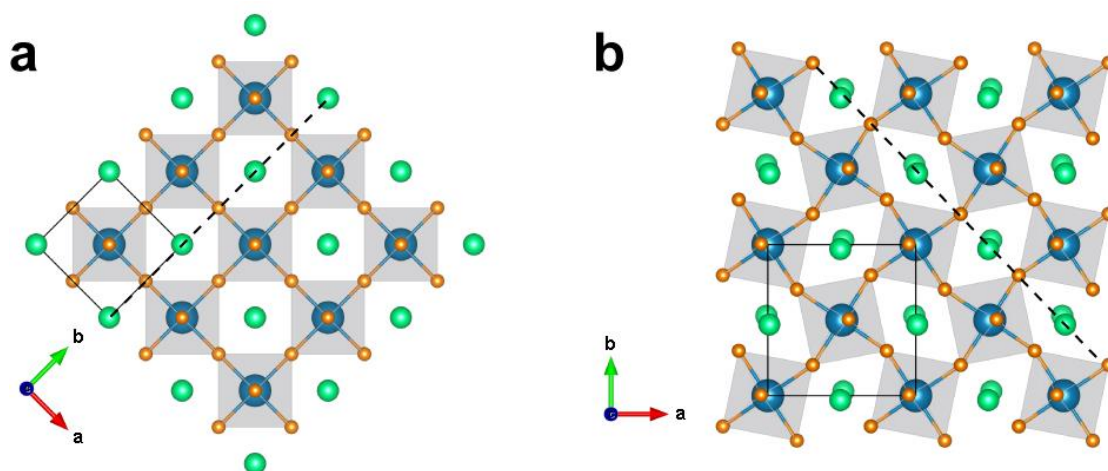


Figure S5. (a) Atomic structure of cubic CsPbBr₃ in the [001] projection (Pm-3m, ICSD #97852) and (b) atomic structure of orthorhombic CsPbBr₃ (Pbnm, ICSD #97851), both viewed along the [001] projection. In the model, the Cs atoms are green, Br atoms orange and Pb are blue, in the center of the light grey octahedra. The conventional cell is indicated by the black lines. The cubic structure is rotated by 45° in the (*a*, *b*) plane for a better comparison. Note that (100) planes in the cubic structure correspond to (110) planes in the Pbnm structure (black dashed lines).

[100] Pnma	↔	[010] Pbnm
[010] Pnma	↔	[001] Pbnm
[001] Pnma	↔	[100] Pbnm
[101] Pnma	↔	[110] Pbnm

Table T2. Relationship between the crystallographic orientations in Pnma and Pbnm orthorhombic settings, reported here for clarity.

6. Results from density functional calculations (vacancies).

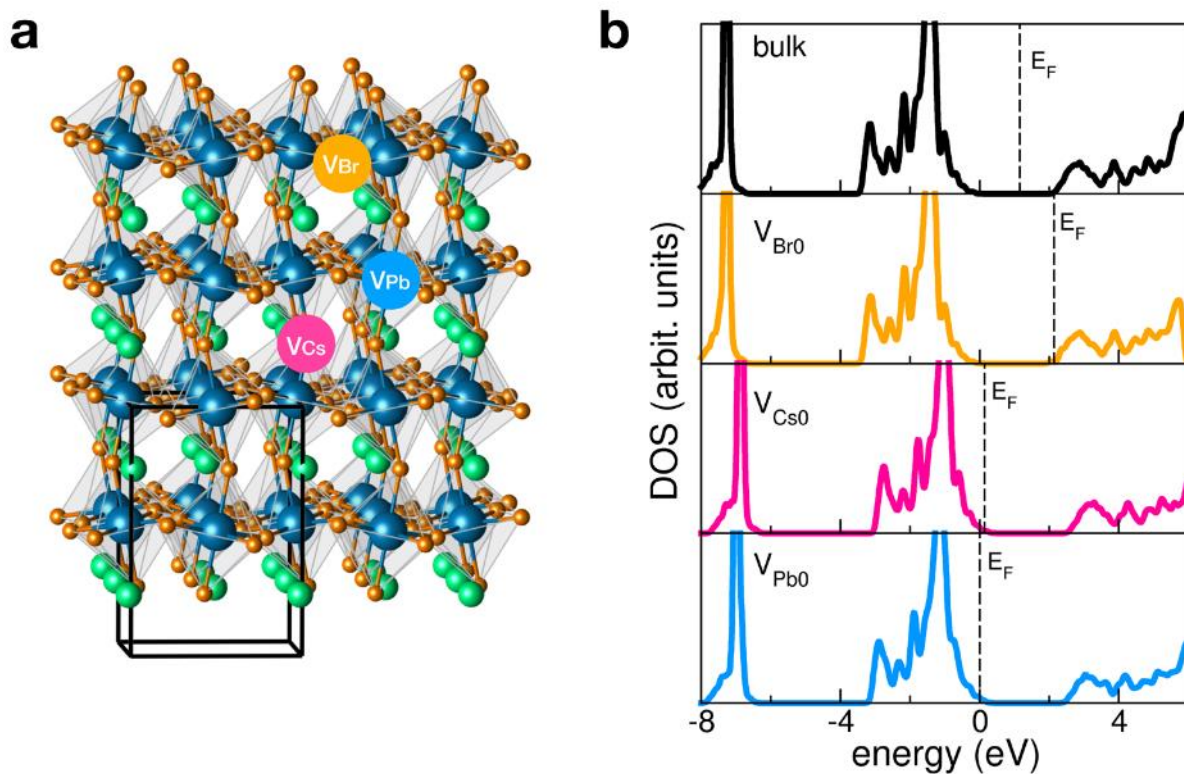


Figure S6. (a) Atomic structure of a $(2 \times 2 \times 2)$ CsPbBr₃ system. Black line marks the unitary cell; colored circles indicated the Cs, Pb and Br atoms removed to simulate the V_{Cs}, V_{Pb} and V_{Br}, respectively. (b) Density of states (DOS) of undefective (bulk) and neutral defective (V_{Cs0}, V_{Pb0} and V_{Br0}) systems. Zero energy reference is set to top of valence band of bulk, vertical dashed lines identify the Fermi level (E_F) of each system. The formation energy of neutral Pb, Cs and Br vacancy in the bulk is 3.3 eV, 4.1 eV, and 3.0 eV, respectively.

7. Experimental loss function.

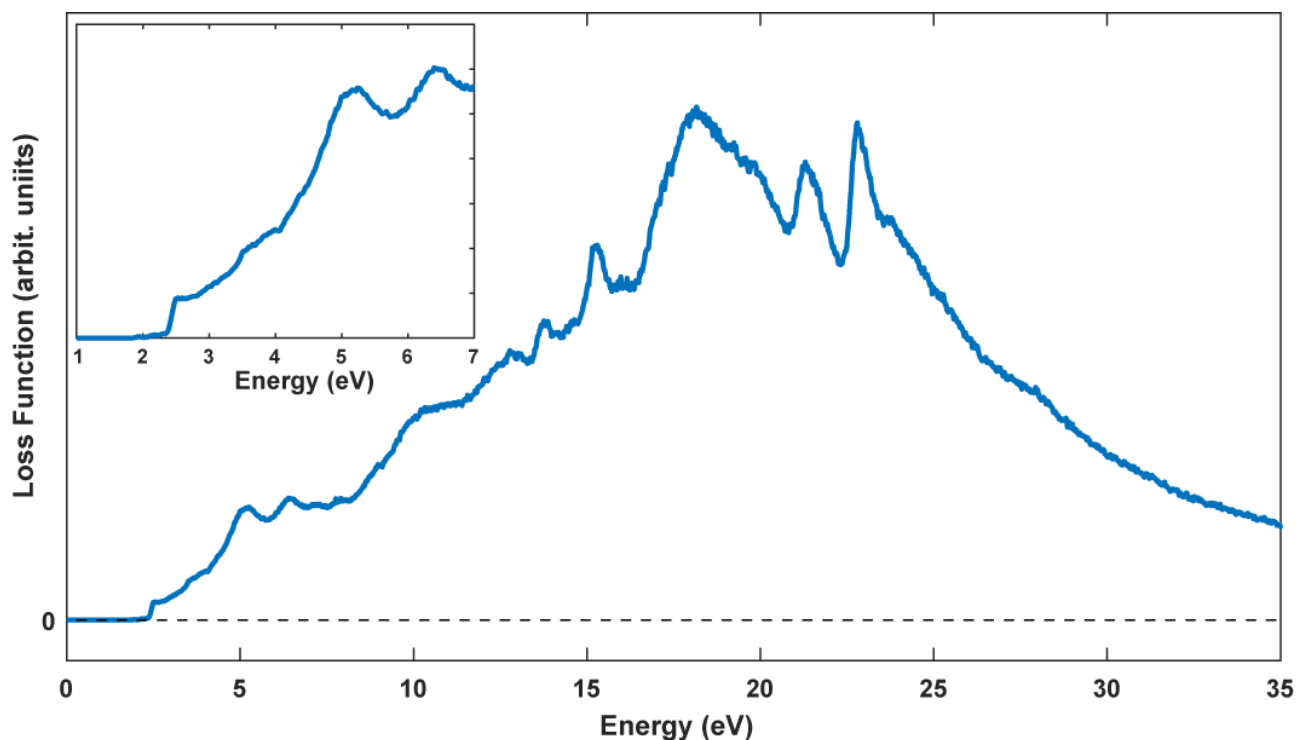


Figure S7. The experimental (bulk) Loss Function of CsPbBr₃ obtained from the thick NS of Figure 4 of the manuscript. The detailed features in the spectrum are a strong indication that the sample was not damaged under the beam.

8. Ultrathin nanosheets ($N \leq 6$).

Ultrathin nanosheets (NSs) with thickness below 3.5 nm ($N \leq 6$) can be obtained with our synthesis, as was demonstrated by our group.² However, their extreme fragility, largely due to the ionic nature of the bonds in this compound, makes it extremely challenging to manipulate them. Ideally, the STEM-EELS analysis has to be performed on nanosheets suspended on a holey carbon film support grid, and the grid must be washed thoroughly, to avoid scattering and absorption from the support films and the surrounding organics affecting the spectra. However, suspending ultrathin NSs on the holes introduces a large tensile stress, resulting in a damage to the crystals. The washing procedure probably introduces additional damage by adding pressure on the suspended crystal (see Figure S8a), which rapidly degrades the NSs to the point that no EELS acquisition in the microscope was possible. The deposition on continuous thin carbon support films did not solve the problem so far (see Figure S8b).

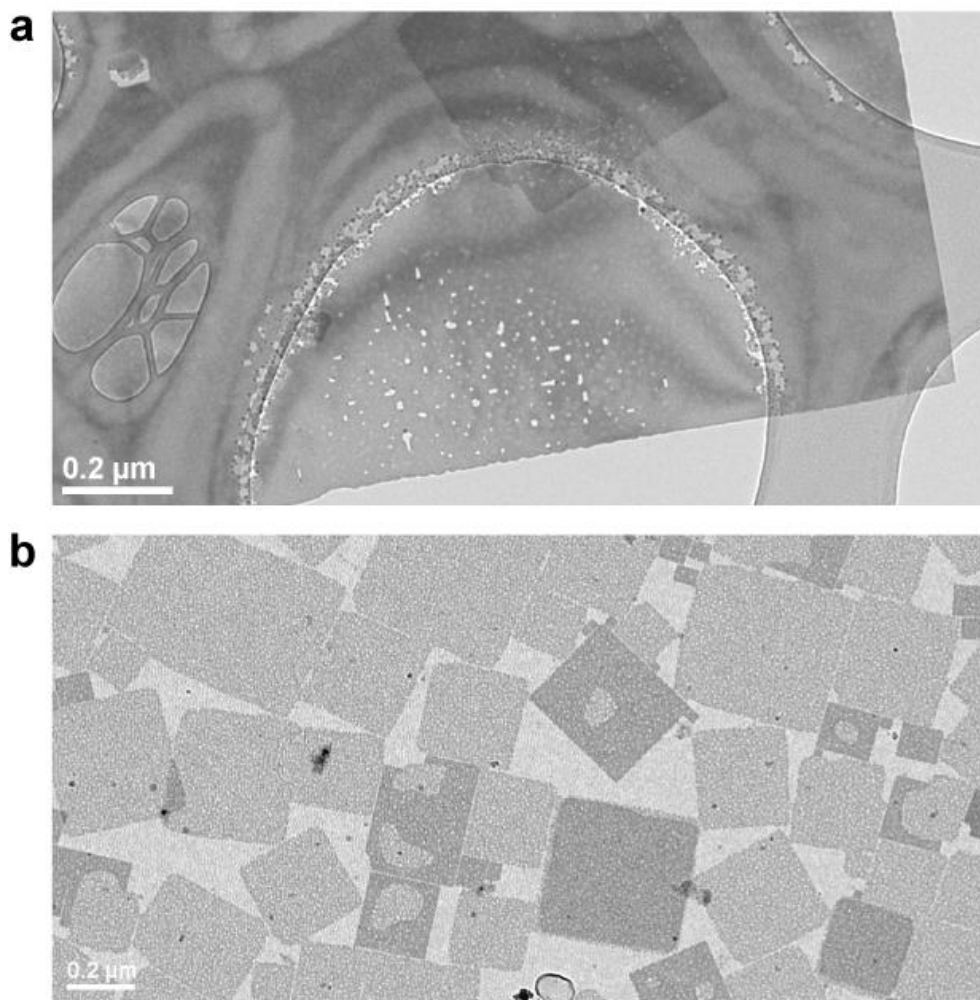


Figure S8. Bright-field TEM image acquired at 100 kV from very thin NSs immediately after synthesis and deposition on the support films. (a) A large NS on a holey carbon support film. (b) Some smaller NSs on a continuous carbon support film. While the NSs look clean and very thin, they present clearly evidences of damage in the form of a porosity distributed everywhere. The images were collected on a JEOL JEM-1011 TEM (Electron Microscopy Facility of IIT, Genova, Italy).

References

1. Z. Dang, J. Shamsi, F. Palazon, M. Imran, Q. A. Akkerman, S. Park, G. Bertoni, M. Prato, R. Brescia and L. Manna, *ACS Nano*, 2017, **11**, 2124-2132.
2. J. Shamsi, Z. Dang, P. Bianchini, C. Canale, F. Di Stasio, R. Brescia, M. Prato and L. Manna, *Journal of the American Chemical Society*, 2016, **138**, 7240-7243.